

Research Article

Distinct Nasopharyngeal and Oropharyngeal Microbiota of Children with Influenza A Virus Compared with Healthy Children

Zhixin Wen ¹, Gan Xie,¹ Qian Zhou,² Chuangzhao Qiu,² Jing Li,¹ Qian Hu,¹ Wenkui Dai,² Dongfang Li,² Yuejie Zheng ¹ and Feiqiu Wen ³

¹Department of Respiratory Diseases, Shenzhen Children's Hospital, No. 7019, Yitian Road, Futian District, Shenzhen 518026, China

²Department of Microbial Research, WeHealthGene Institute, 3C19, No. 19 Building, Dayun Software Town, Shenzhen 518000, China

³Department of Hematology and Oncology, Shenzhen Children's Hospital, Shenzhen 518038, China

Correspondence should be addressed to Feiqiu Wen; fwen62@126.com

Received 22 July 2018; Revised 24 October 2018; Accepted 6 November 2018; Published 19 November 2018

Academic Editor: Paul M. Tulkens

Copyright © 2018 Zhixin Wen et al. This is an open access article distributed under the Creative Commons Attribution License, which permits unrestricted use, distribution, and reproduction in any medium, provided the original work is properly cited.

Background. Influenza A virus (IAV) has had the highest morbidity globally over the past decade. A growing number of studies indicate that the upper respiratory tract (URT) microbiota plays a key role for respiratory health and that a dysfunctional respiratory microbiota is associated with disease; but the impact of microbiota during influenza is understudied. **Methods.** We recruited 180 children, including 121 IAV patients and 59 age-matched healthy children. Nasopharyngeal (NP) and oropharyngeal (OP) swabs were collected to conduct 16S rDNA sequencing and compare microbiota structures in different individuals. **Results.** Both NP and OP microbiota in IAV patients differed from those in healthy individuals. The NP dominated genera in IAV patients, such as *Moraxella*, *Staphylococcus*, *Corynebacterium*, and *Dolosigranulum*, showed lower abundance than in healthy children. The *Streptococcus* significantly enriched in patients' NP and *Phyllobacterium* could be generally detected in patients' NP microbiota. The most abundant genera in OP microbiota showed a decline tendency in patients, including *Streptococcus*, *Neisseria*, and *Haemophilus*. The URT's bacterial concurrence network changed dramatically in patients. NP and OP samples were clustered into subgroups by different dominant genera; and NP and OP microbiota provided the precise indicators to distinguish IAV patients from healthy children. **Conclusion.** This is the first respiratory microbiome analysis on pediatric IAV infection which reveals distinct NP and OP microbiota in influenza patients. It provides a new insight into IAV research from the microecology aspect and promotes the understanding of IAV pathogenesis.

1. Introduction

Various respiratory viral agents, such as influenza A virus (IAV), adenovirus (ADV), and respiratory syncytial virus (RSV), are common pathogens which cause childhood community-acquired pneumonia (CAP) [1]. In the past ten years, influenza has caused a high morbidity ratio in China and other countries globally, especially in 2017-2018 [2, 3]. Several studies reported on the mechanisms of IAV, such as virulence [4], evolution [5], and host-virus interaction [6]. However, only a few studies reported microbiome changes during influenza infection and these were mainly conducted in adult or aged populations [7–10].

The upper respiratory tract (URT) functions as an interface between exterior environments, lung and gastrointestinal tract [11], and primes the host immune system to protect the mucosal surface from pathogenic infection [12, 13]. Several reviews summarized the viral-bacterial superinfection pathway [14, 15], which indicate that microbiota dysbiosis is associated with pathogen invasion, escaping the host immune system and finally leading to respiratory disease.

Recently, several reports have indicated that healthy and diseased children have different nasopharyngeal (NP) and oropharyngeal (OP) microbiota [16–18]. Moreover, this distinct respiratory microbiota pattern varied with infectious pathogens [19]. For instance, the health-associated

commensals *Corynebacterium* and *Dolosigranulum* are significantly decreased in *Mycoplasma pneumoniae* pneumonia patients [18]. Dominant *Haemophilus/Streptococcus* in NP microbiota indicate a high risk of respiratory infection [20] or more severe bronchiolitis [21]. RSV patients' microbiota in the respiratory tract also revealed a significant alteration [22], with dominant *Streptococcus pneumoniae* and *Staphylococcus aureus* associated with historical IAV pandemics [23]. Furthermore, Wouter *et al.* demonstrated that the abundant lactobacilli, *Rothia* or *S. pneumoniae*, were positively related to pneumonia severity index (PSI) [16].

These findings suggest the importance of the bacterial community during respiratory viral infection. However, how the bacterial community of the URT changes in pediatric IAV remains to be explored. In this study, we investigated NP and OP microbiota using 16S-based sequencing and aimed to identify alterations in IAV patients compared to healthy children. Bacterial markers to distinguish IAV patients and healthy children were also explored.

2. Materials and Methods

2.1. Ethical Approval. This study was approved by the Ethical Committee of Shenzhen Children's Hospital (registration number 2016013). Guardians of recruited children provided informed consent. All procedures performed in this study were in accordance with ethical standards of the institutional and/or national research committee, as well as the 1964 Helsinki declaration and its subsequent amendments, or comparable ethical standards.

2.2. Subjects Inclusion and Pathogen Detection. All children with suspected IAV infection were enrolled at the fever outpatient clinic at Shenzhen Children's Hospital. Patients with confirmed IAV who met the following criteria were selected: (i) typical clinical symptoms of acute influenza (fever, cough, dyspnea, and vomiting); (ii) positive detection of IAV by rapid PCR-fluorescence probing (DaAnGene, Guangzhou, China); (iii) no antibiotic administration before fever clinic; (iv) severe cases, defined by severity of symptoms and those who were admitted to the intensive care unit (ICU).

NP microbial samples were collected by skilled clinicians during the outpatient evaluation with specific swabs (25-800-A-50, Puritan, Guilford, North Carolina, USA). At the same time, OP microbial samples were also collected by specific swabs (155C, COPAN, Murrieta, USA) [24]. Common pathogens were detected by the following methods: bacterial culturing was conducted to detect clinical common bacterial pathogens [25] and nucleic acid testing (NAT) was applied to identify viral or atypical pathogens as described previously [18]. Unused swabs and DNA extraction kits were utilized as negative controls to assess for experimental contamination [18]. All specimens were frozen at -80°C for microbial sequencing.

Healthy children were recruited after physical examination at Shenzhen Children's Hospital [24], according to the following criteria: no asthma or family history of allergy; no history of pneumonia; no wheezing, fever, cough, or other respiratory/allergic symptoms; no antibiotic exposure for 1

month prior to this study; and no disease symptoms within 1 week of sampling.

2.3. DNA Extraction, PCR, and Sequencing. Microbial genomic DNA was extracted using the Power Soil DNA Isolation Kit (Mo Bio Laboratories, Carlsbad, CA, USA). PCR amplicon libraries were constructed by the V3-V4 hypervariable region of the 16S rDNA gene [26]. Qualified libraries were then sequenced by the Illumina MiSeq sequencing platform (Illumina, San Diego, CA, USA) [27].

2.4. Bioinformatics Analysis and Visualization. Raw sequencing data were processed by the QIIME pipeline [28]. Data filtration, representative taxa assignment, and diversity calculations were conducted according to our previous study [29]. A rarefaction curve of OTU was used to assess the saturation of sequencing data. Principal component analysis (PCA) was used to distinguish IAV samples from healthy ones. The statistical difference of characters between patients and healthy children was using chi-square test (p value). The comparison of bacterial relative abundance between patients and healthy children was performed by Wilcoxon rank-sum test and the significance of multiple comparisons was adjusted by FDR (q -value). Distances between samples were calculated by Bray-Curtis dissimilarity and then clustered by the hierarchical method. The visualization of cluster topology used iTol [30], and the best subgroup was divided by the Silhouette method. The community concurrence network was constructed based on the correlation of microbiota by Spearman's rank correlation coefficient [18]. The prediction model was selected by the random forest method and cross-validation was used to select biomarkers for predicting disease versus health [31]. Receiver-operating characteristic (ROC) curves and the area under the curve (AUC) for each crucial genus were applied to assess the accuracy of biomarkers [9]. All other data visualization was produced by the package "ggplot2" of R software (v. 3.2.3) and Cytoscape (v. 3.4.0).

3. Results

3.1. Sample Information, Data Output, and Confounder Analysis. We enrolled 180 children, including 121 patients with IAV and 59 age-matched healthy children. Patients with IAV had no history of allergy, pneumonia, or asthma. Characteristics of the study population are summarized in Table 1. Based on disease severity, 11 patients were classified as severe and admitted to the pediatric ICU (Table S1). The confounder analysis indicated that IAV infection is the most significant factor to explain variations in microbial samples.

A total of 9,018,174 high-quality tags were produced, averaging 25,592 (6,911–29,192), 26,596 (17,368–29,218), 26,063 (18,303–29,272), and 21,493 (9,724–28,738) for the NP-IAV (NP-P), OP-IAV (OP-P), NP-health (NP-H), and OP-health (OP-H) groups, respectively. The average OTU numbers in the NP-P, OP-P, NP-H, and OP-H groups were 1,004, 383, 255, and 143, respectively (Supplementary Figure 1).

3.2. NP and OP Microbiota of Patients Differ Significantly from Those of Healthy Children. The diversity of the microbial

TABLE 1: Sample information.

	Healthy Children (n = 59)	IAV Patients (n = 121)	P-value
<i>Characteristics</i>			
<i>Gender</i>			
Female	33(55.9%)	47(38.8%)	0.045
Male	26(44.1%)	74(61.2%)	
Age (years)*	2.8(0.1–9.9)	2.9(0.1–13.8)	
<i>Delivery Mode</i>			
Caesarean section	20(33.9%)	39(32.2%)	0.365
Vaginally born	39(66.1%)	82(67.8%)	
<i>Feed Pattern</i>			
Breast feed	18(30.5%)	68(56.2%)	0.004
Breast feed + Milk feed	31(52.5%)	42(34.7%)	
Milk feed	10(16.9%)	11(9.1%)	
Family history of allergy	-	-	
History of pneumonia	-	-	
Asthma	-	-	
<i>Clinical records</i>			
Fever	-	116(95.9%)	
Fever duration(days)*	-	2(1-12)	
Cough	-	83(68.6%)	
Cough duration(days)*	-	2(1-30)	
WBC (5-12%)	NA	80(66.1%)	
hsCRP (≤ 0.5 mg/l)	NA	26(21.5%)	
PCT (< 0.5 ng/ml)	NA	61(50.4%)	

“NA” represents not available; CRP, C-reactive protein; PCT, Procalcitonin; “-” represents not detected; “*”: this feature is described with median (range).

community in the NP-P/OP-P group was significantly higher than that of the NP-H/OP-H group (p value < 0.001) (Figure 1(a)). The diversity of the OP microbiota was also higher than that of the NP microbiota, in both healthy and diseased children (Figure 1(a)). Microbial samples in patients with IAV were clearly separated in clustering compared to healthy controls (Figures 1(b) and 1(c)).

Firmicutes predominates in both the NP and OP microbiota of healthy or diseased children (NP: 39.17% in IAV patients vs. 43.14% in healthy children, q -value=0.594; OP: 47.27% in IAV patients vs. 46.50% in healthy children, q -value=0.730) (Table S2). Proteobacteria accounts for a secondary proportion of NP microbiota in the disease group. On the contrary, the abundance of Proteobacteria was significantly lower in the OP-P group (q -value=0.030). Actinobacteria significantly changed in both NP (q -value=0.023) and OP (q -value =0.001) microbiota during IAV infection (Table S2).

At the genus level, the abundant *Moraxella* of NP exhibited a decline tendency in IAV patients compared to healthy children, followed by *Staphylococcus* (q -value=0.018), *Corynebacterium*, and *Dolosigranulum* (Figure 1(d), Table S3). On the other hand, *Streptococcus* was enriched significantly in NP-P (16.79% vs. 10.09% in NP-H, q -value=0.028) while *Phyllobacterium* could only be detected in patients with IAV (6.94% vs. 0.00% in NP-H, q -value < 0.001) (Figure 1(d), Table S3). Other dominant genera such as *Acinetobacter*,

unclassified *Acidobacteria*, *Ralstonia*, *Pseudomonas*, *Lachnospirillum*, and *Halomonas* increased significantly in the IAV group (Figure 1(d), Table S3).

In OP microbiota, seven of the top 10 genera showed lower abundance in patients, including *Streptococcus*, *Neisseria* (13.06% vs. 6.05%, q -value=0.017), *Haemophilus* (6.29% vs. 1.59%, q -value < 0.001), *Rothia* (4.34% vs. 3.08%, q -value=0.045), *Fusobacterium*, *Granulicatella* (2.11% vs. 0.68%, q -value < 0.001), and *Gemella*. The remaining three genera, *Prevotella*, *Veillonella*, and *Leptotrichia*, were amassed during IAV infection (Figure 1(e), Table S3). *Lactobacillus*, *Eubacterium*, *Atopobium*, and *Actinomyces* show a significant increment in ED (Figure 1(e), Table S3).

3.3. NP and OP Concurrence Bacterial Network Altered in Patients. In NP-H, the concurrence bacterial network (Figure 2) consisted of 34 genera and could be grouped into two subnetworks with three hub nodes, namely, *Prevotella*, *Roseburia*, and *Bacteroides*. However, the NP microbial interaction shaped to a more complex network with more but different genera (44 genera; 16 genera also represented in NP-H). The structure of the microbial interaction in the OP tended to be simpler and linear during influenza onset (Figure 2).

3.4. Different Composition of Microbiota in Subclusters of NP and OP, but No Specific Pattern Related to Severe Case.

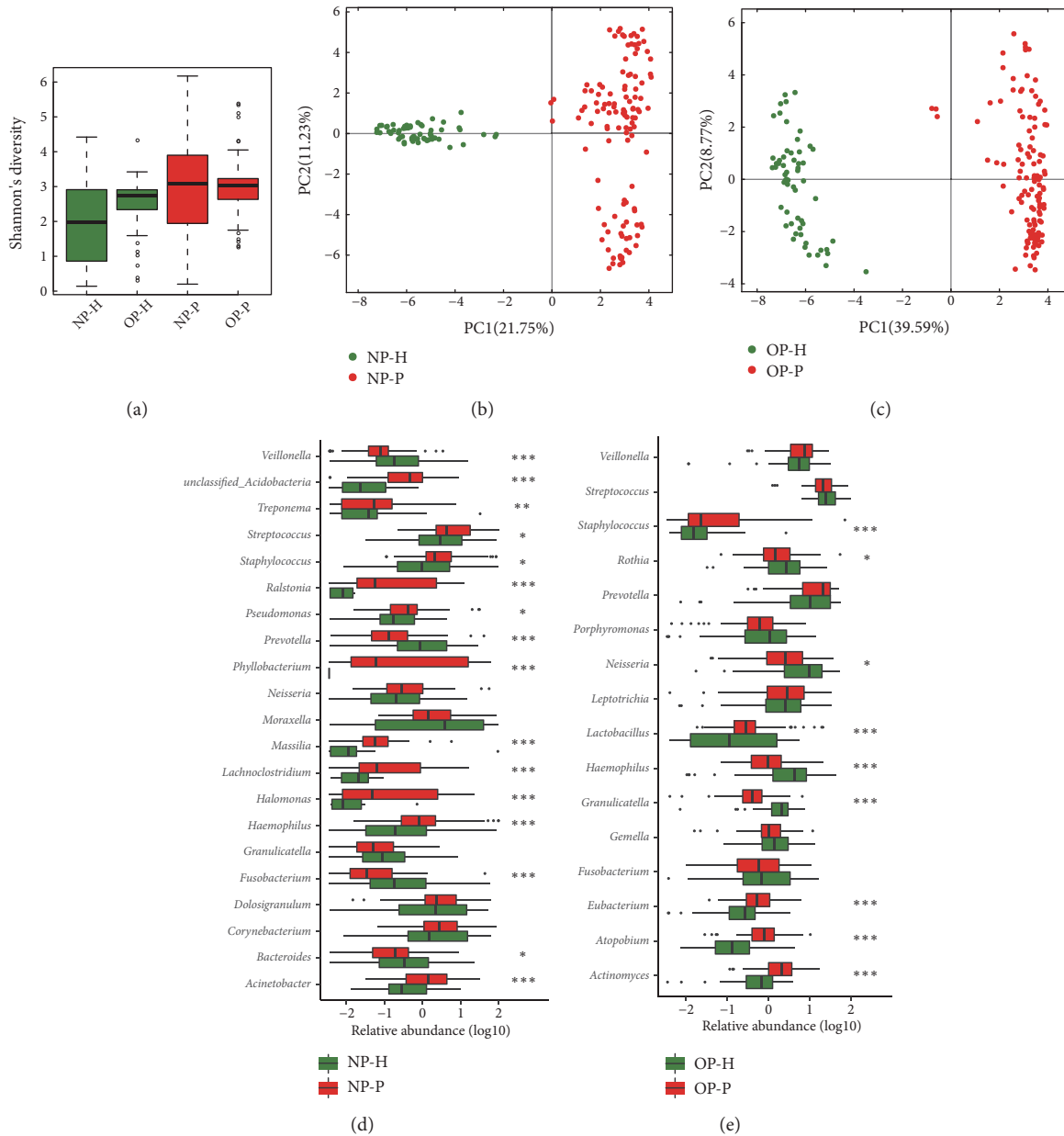


FIGURE 1: NP/OP microbiota structure in IAV patients and healthy children. (a) Shannon index of NP and OP microbiota in patients and healthy children. (b, c) Principal components analysis (PCA) of NP/OP samples. (d, e) Comparison of dominated genera of NP/OP microbiota between patients with IAV and healthy children. The vertical axis represents genus name, and the horizontal axis shows the log₁₀ value of relative abundance. *, **, and *** represent *q*-values ≤ 0.05 , ≤ 0.01 , and ≤ 0.001 , respectively. Objects painted green or red represent healthy or disease samples.

With hierarchical clustering, NP samples could be divided into 6 subsets (G1 to G6) (Figure 3(a)), except that the two subbranches consist of only one or two samples. The dominated genera in each subset are *Haemophilus* (66.05%, G1 contains 6 samples), *Streptococcus* (63.77%, G2 contains 24 samples), *Staphylococcus* (65.80%, G3 contains 6 samples), mixed *Corynebacterium-Dolosigranulum* (39.22% and 24.95%, G4 contains 15 samples), *Moraxella* (45.16%, G5 contains 12 samples), and mixed *Zoogloea-Phyllobacterium* (24.93% and 13.85%, G6 includes 51 samples). Although

OP samples could not be clearly separated into subclusters, several patterns of specific bacterial components were recognized, such as *Streptococcus*-dominant, *Prevotella*-dominant, and mixed genera with several dominating (Figure 3(b)). The 11 severe cases admitted to the ICU included P1, P3, and P32 assigned to G2, P53 to G4, P111 in the small branch (with only two samples), and the other six patients (P2, P23, P56, P88, P103, and P110) to G6. There was no correlation between disease severity and bacterial composition, and no relevant genus related to severe illness.

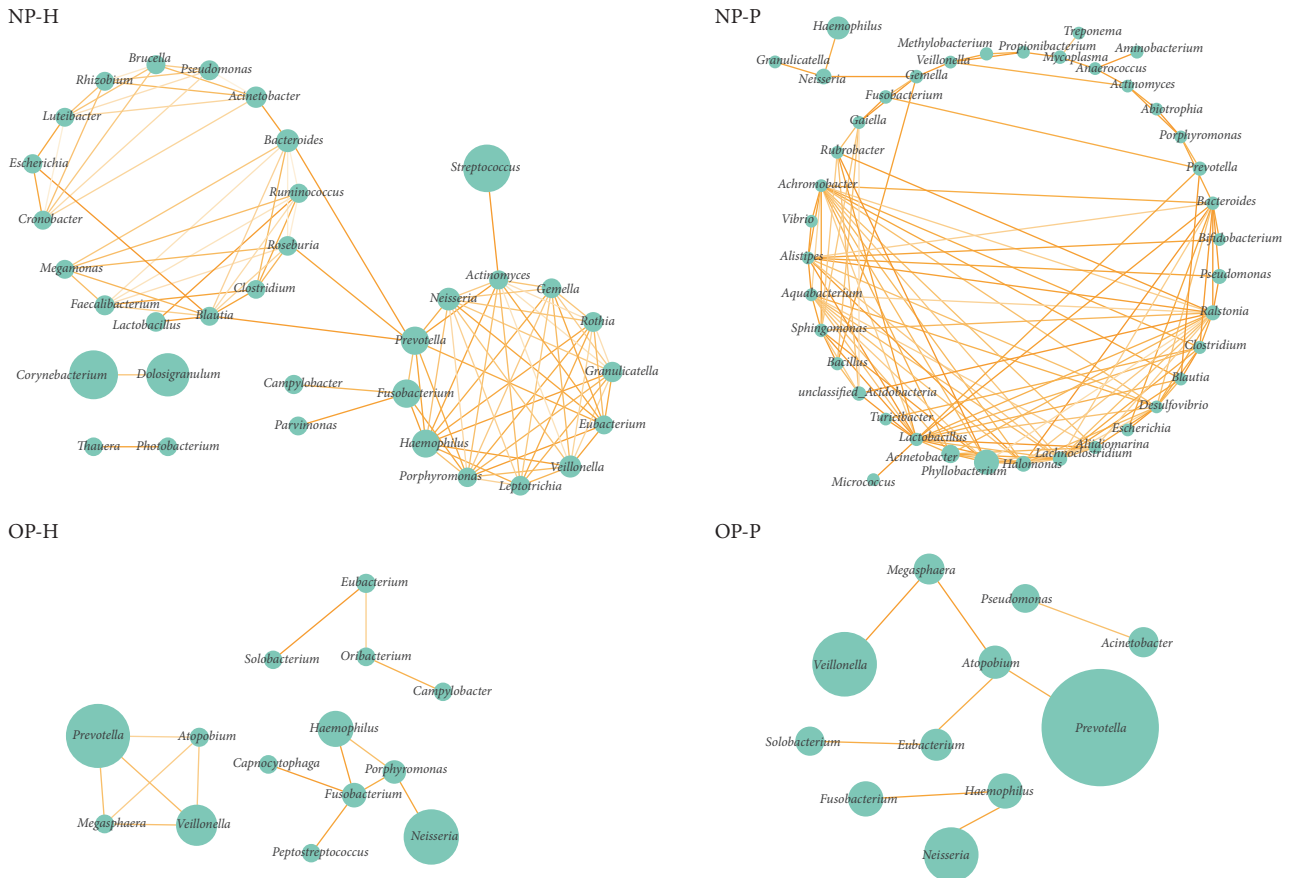


FIGURE 2: Co-occurrence network of NP/OP microbiota in patients with IAV and healthy ones. The circle size represents relative abundance, and the density of the dashed line represents the Spearman coefficient.

3.5. Key Genera Served as Biomarkers to Provide Prediction Model for IAV Infection. Key genera were identified by random forest analysis to distinguish patients with IAV from healthy controls based on URT microbiota composition. After cross-validation, five NP genera, including *Cronobacter*, *Luteibacter*, *Azonexus*, *Rubrobacter*, and *Turicibacter*, were found to be the most important indicators to discriminate between patients with IAV and healthy controls, with greater predictive efficiency (AUC values of 0.967, 0.963, 0.940, 0.947, and 0.942, respectively) (Figure 4(a)). In the OP microbiota, 19 genera were identified as biomarkers, and nine of those showed high accuracy (AUC > 0.900) (Figure 4(b)), especially for *Lachnoanaerobaculum* (AUC = 0.973) (Figure 4(b)).

4. Discussion

The respiratory tract is colonized by various microbes [32], plays an important immune function during childhood, and is a defender against pathogen invasion [33, 34]. During respiratory infection, the microecology becomes unstable, resulting in dysbiosis of the virus-bacteria community [14]. NP microbial commensals primarily extract barren nutrients from the respiratory epithelium [35] and are easily influenced by the exterior environment [36]. The diversity of NP microbiota significantly increased in patients with IAV

compared to healthy children, but decreased in bacterial respiratory infection [37, 38]. This may be due to virus-specific characters, such as suppressing bacterial clearance, inflow of nutrients, and promotion of bacterial outgrowth [15]. Contrary to the NP, the OP microbial environment is abundant with nutrition due to food ingestion and esophageal reflux, which implicates a more stable and massive microbiota than that of the NP niche [39, 40]. Therefore, the diversity of the OP microbiota shows a nonobvious changing tendency in patients with IAV. This can be partly explained by specific clearance mechanisms for different pathogens in different respiratory niches [41].

The predominant *Corynebacterium* and *Dolosigranulum* in the NP microbiota were strongly associated with a reduced ratio of acute otitis media [42], which have shown decline tendency in IAV patients. *Moraxella*, which is associated with lower risk of respiratory infection [34], also occupied lower abundance in patients than in healthy children. On the contrary, *Streptococcus* has been shown to be the most abundant, by synergistic stimulation of type I interferons during influenza virus infection [43] and resulting in pneumonia susceptibility [32]. The suddenly enriched *Phyllobacterium*, which could not be detected in healthy NP samples, have not been reported in human diseases until now. The OP bacterial community also changed dramatically and is inconsistent

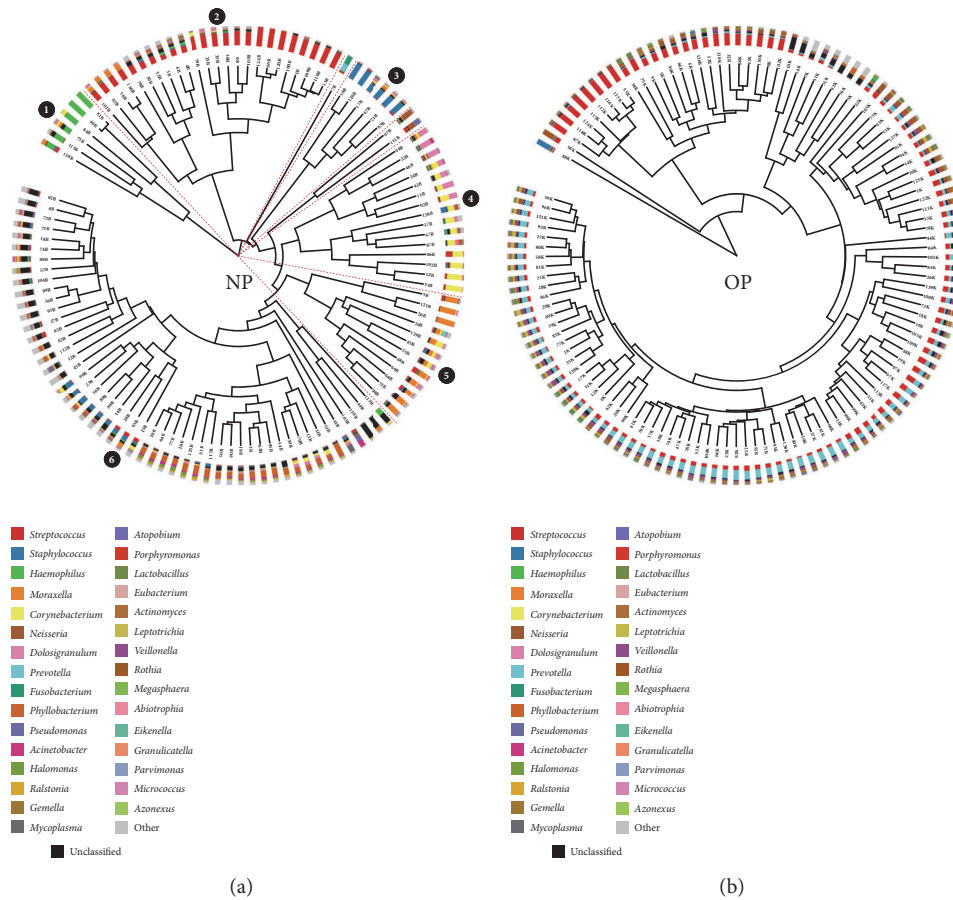


FIGURE 3: Hierarchical clustering analysis of microbiota in the NP and OP. The circle dendrograms were constructed based on the dissimilarity of microbiota composition between samples. Adjacent to the dendrogram branch ends, stacked bar charts show the relative abundance of the dominant genera in the NP and OP. Subclusters (defined as more than three samples) are designated by the dotted red lines originating from the center of the dendrogram.

with a previous adult IAV microbiota study [9], in which *Bacteroidetes* is the most abundant, whether in healthy or diseased patients, followed by *Proteobacteria* and *Firmicutes*. It is implicated to have a different composition in children and adults during the aging process [44]. As a result, the core bacterial concurrence network was reconstructed unrecognizably in the NP and is simpler in the OP of IAV children.

According to recent studies, the microbiota can be further divided into subgroups. Alexandre et al. indicated that patients with IAV represent individual specific microbiota compositions [10]. Adults or elderly patients can be clustered into several subgroups, whose URT microbiota dominated by *Streptococcus* was strongly associated with the pneumonia severity index [16]. In our study, NP microbiota was also separated into subgroups with group-specific dominated bacteria, but no specific pattern related to the severe cases.

Luna et al. indicated that the nasal microbiota could be used to detect disease severity [45]. In this study, we also found microbial indicators to precisely distinguish those with IAV and healthy children. Until now, neuraminidase inhibitors, such as the well-known oseltamivir, were recommended to treat and prevent influenza, although with an

increased risk of side effects [46]. Although the vaccination is currently the best prevention method, we also noticed that mispredicted pandemic influenza strains over the past year led to a worldwide medical burden. On the other hand, the rapid evolution of influenza could disable the preexisting vaccination [47]. Combining valuable biomarkers with the microbial characteristics of other pediatric URTs will provide more comprehensive information for influenza prevention and prediction.

There were several limitations to this study. No precise types of IAV strains were reported due to the clinical practice of using a generic influenza A virus detection kit; this might have partly impacted the NP subgroups' microbiota composition. Also, all samples were collected when patients first presented to the fever clinic; we could not determine patterns existing between severe cases and mild cases. Though we identified predictive indicators to distinguish IAV and healthy individuals, it might be difficult to identify IAV among other respiratory virus infections. Lastly, 16S rDNA analysis cannot identify species-level pathogens, nor explain functional dysbiosis in the infection-caused microbiota disorder.

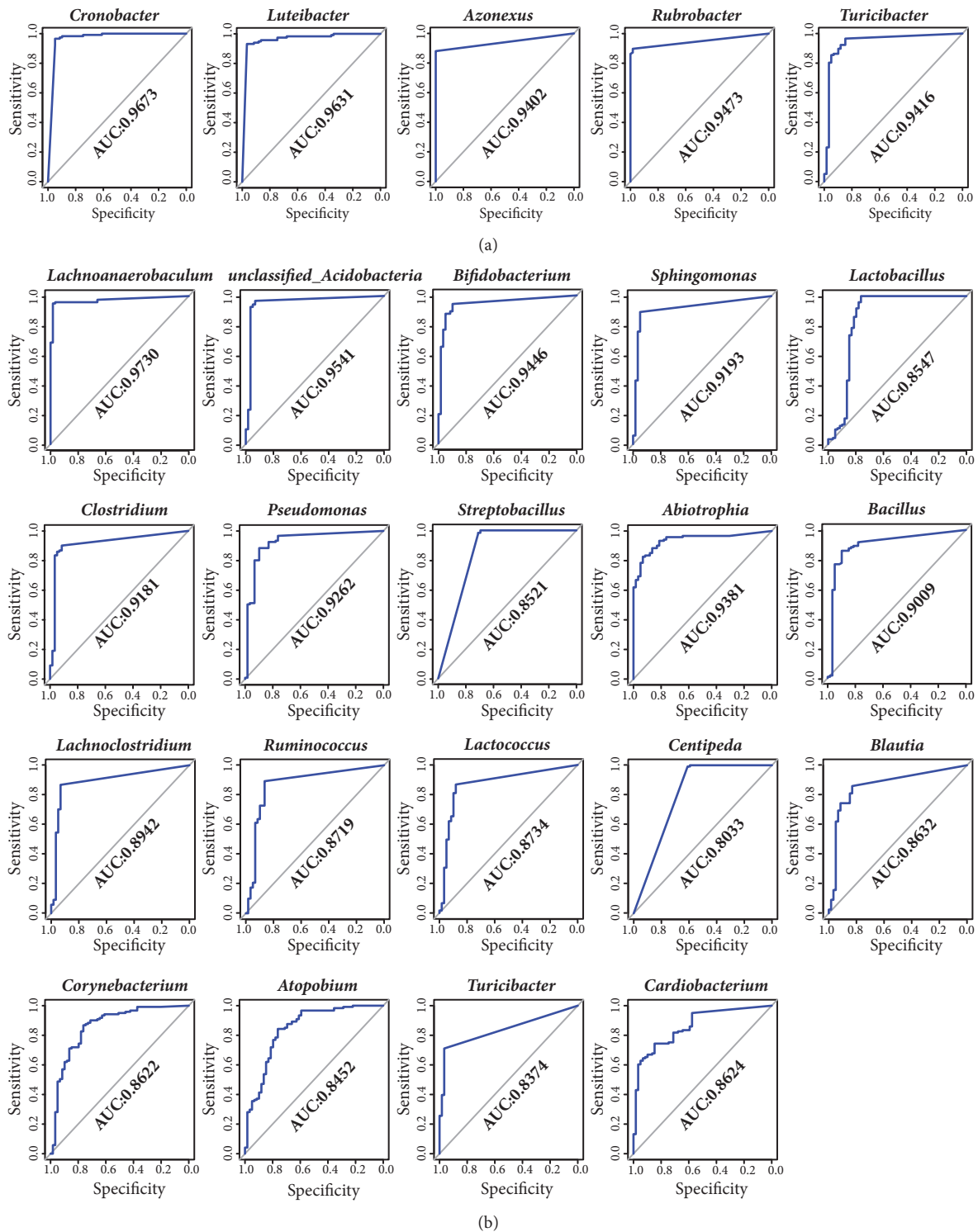


FIGURE 4: Prediction of biomarkers in the NP/OP microbiome. Receiver-operating characteristic (ROC) plots were used to estimate the efficiency of five key genera in NP (a) and 19 key genera in OP (b). The area under curve (AUC) of each genus shows the high accuracy to distinguish patients with IAV from healthy controls.

5. Conclusions

This study is the first research on the microbiota of pediatric patients with IAV infection and is thus an important reference for understanding the respiratory microbiota in this population. These findings reveal the dysbiosis of the microbiota of URTs in children with IAV and provide new insight into the pathogenesis of IAV.

Data Availability

The 16S sequencing data used to support the findings of this study have been deposited in the GenBank repository under accession numbers SRP090593 (healthy children) and SRP149307 (children with IAV).

Conflicts of Interest

The authors declare that they have no conflicts of interest.

Authors' Contributions

Feiqiu Wen and Zhixin Wen managed the project. Gan Xie, Jing Li, and Qian Hu selected the patients, collected the samples, and performed the clinical detection. Qian Zhou and Chuangzhao Qiu performed the bioinformatics analysis and optimized the graphs. Zhixin Wen and Gan Xie interpreted the results and wrote the paper. Wenkui Dai and Dongfang Li polished the article. Yuejie Zheng provided professional suggestions. All authors reviewed this manuscript. Zhixin Wen and Gan Xie contributed equally.

Acknowledgments

This work was supported by the Key Medical Disciplines Building Project of Shenzhen (SZXJ2018043) and Shenzhen public service platform for clinical drug trials (20151964).

Supplementary Materials

Supplementary Material 1. Table S1: sample information of patients with influenza A virus and healthy children. Table S2: Wilcoxon rank-sum test results of the NP and OP at the phylum level between patients with IAV and healthy children. Table S3: Wilcoxon rank-sum test result of the NP and OP at the genus level between patients with IAV and healthy children. Table S4: detailed genus profile of all samples.

Supplementary Material 2. Figure S1: the rarefaction of samples shows the sequencing data is saturated.

References

- [1] J. S. Bradley, C. L. Byington, S. S. Shah et al., "The management of community-acquired pneumonia in infants and children older than 3 months of age: Clinical practice guidelines by the pediatric infectious diseases society and the infectious diseases society of America," *Clinical Infectious Diseases*, vol. 53, no. 7, pp. e25–e76, 2011.
- [2] J. Artois, H. Jiang, X. Wang et al., "Changing geographic patterns and risk factors for avian influenza A(H7N9) infections in humans, China," *Emerging Infectious Diseases*, vol. 24, no. 1, pp. 87–94, 2018.
- [3] "Recommendations for Prevention and Control of Influenza in Children, 2017 – 2018," *Pediatrics*, vol. 140, no. 4, p. e20172550, 2017.
- [4] X. Gong, H. Yin, Y. Shi et al., "Evaluation of the immunogenicity and protective effects of a trivalent chimeric norovirus P particle immunogen displaying influenza HA2 from subtypes H1, H3 and B," *Emerging microbes & infections*, vol. 5, p. e51, 2016.
- [5] S. Zou, R. Gao, Y. Zhang et al., "Molecular characterization of H6 subtype influenza viruses in southern China from 2009 to 2011," *Emerging microbes & infections*, vol. 5, no. 7, p. e73, 2016.
- [6] E. J. A. Schrauwen and R. A. M. Fouchier, "Host adaptation and transmission of influenza A viruses in mammals," *Emerging Microbes and Infections*, vol. 3, 2014.
- [7] R. K.-K. Leung, J.-W. Zhou, W. Guan, S.-K. Li, Z.-F. Yang, and S. K.-W. Tsui, "Modulation of potential respiratory pathogens by pH1N1 viral infection," *Clinical Microbiology and Infection*, vol. 19, no. 10, pp. 930–935, 2013.
- [8] B. Chaban, A. Albert, M. G. Links et al., "Characterization of the Upper Respiratory Tract Microbiomes of Patients with Pandemic H1N1 Influenza," *PLoS ONE*, vol. 8, no. 7, p. e69559, 2013.
- [9] H. Lu, A. Li, T. Zhang et al., "Disordered oropharyngeal microbial communities in H7N9 patients with or without secondary bacterial lung infection," *Emerging Microbes & Infections*, vol. 6, no. 12, p. e112, 2017.
- [10] A. L. Greninger, E. C. Chen, T. Sittler et al., "A Metagenomic Analysis of Pandemic Influenza A (2009 H1N1) Infection in Patients from North America," *PLoS ONE*, vol. 5, no. 10, p. e13381, 2010.
- [11] A. Sahin-Yilmaz and R. M. Naclerio, "Anatomy and physiology of the upper airway," *Proceedings of the American Thoracic Society*, vol. 8, no. 1, pp. 31–39, 2011.
- [12] P. G. Holt, D. H. Strickland, M. E. Wikström, and F. L. Jahnsen, "Regulation of immunological homeostasis in the respiratory tract," *Nature Reviews Immunology*, vol. 8, no. 2, pp. 142–152, 2008.
- [13] T. J. Braciale, J. Sun, and T. S. Kim, "Regulating the adaptive immune response to respiratory virus infection," *Nature Reviews Immunology*, vol. 12, no. 4, pp. 295–305, 2012.
- [14] S. V. Lynch, "Viruses and microbiome alterations," *Annals of the American Thoracic Society*, vol. 11, no. 1, pp. S57–S60, 2014.
- [15] J. C. Brealey, P. D. Sly, P. R. Young, and K. J. Chappell, "Viral bacterial co-infection of the respiratory tract during early childhood," *FEMS Microbiology Letters*, vol. 362, no. 10, 2015.
- [16] W. A. A. De Steenhuijsen Piters, E. G. W. Huijskens, A. L. Wyllie et al., "Dysbiosis of upper respiratory tract microbiota in elderly pneumonia patients," *The ISME Journal*, vol. 10, no. 1, pp. 97–108, 2016.
- [17] O. Sakwinska, V. B. Schmid, B. Berger et al., "Nasopharyngeal microbiota in healthy children and pneumonia patients," *Journal of Clinical Microbiology*, vol. 52, no. 5, pp. 1590–1594, 2014.
- [18] Z. Lu, W. Dai, Y. Liu et al., "The alteration of nasopharyngeal and oropharyngeal microbiota in children with MPP and non-MPP," *Gene*, vol. 8, no. 12, 2017.
- [19] S. Bousbia, L. Papazian, P. Saux et al., "Repertoire of Intensive Care Unit Pneumonia Microbiota," *PLoS ONE*, vol. 7, no. 2, p. e32486, 2012.
- [20] A. A. T. M. Bosch, E. Levin, M. A. van Houten et al., "Development of upper respiratory tract microbiota in infancy is affected by mode of delivery," *EBioMedicine*, vol. 9, pp. 336–345, 2016.

- [21] K. Hasegawa, J. M. Mansbach, N. J. Ajami et al., "Association of nasopharyngeal microbiota profiles with bronchiolitis severity in infants hospitalised for bronchiolitis," *European Respiratory Journal*, vol. 48, no. 5, pp. 1329–1339, 2016.
- [22] Q. Hu, W. Dai, Q. Zhou et al., "Dynamic oropharyngeal and faecal microbiota during treatment in infants hospitalized for bronchiolitis compared with age-matched healthy subjects," *Scientific Reports*, vol. 7, no. 1, 2017.
- [23] A. Rynda-Apple, K. M. Robinson, and J. F. Alcorn, "Influenza and bacterial superinfection: Illuminating the immunologic mechanisms of disease," *Infection and Immunity*, vol. 83, no. 10, pp. 3764–3770, 2015.
- [24] Heping Wang, Wenkui Dai, Xin Feng et al., "Microbiota Composition in Upper Respiratory Tracts of Healthy Children in Shenzhen, China, Differed with Respiratory Sites and Ages," *BioMed Research International*, vol. 2018, Article ID 6515670, 8 pages, 2018.
- [25] M. M. Pettigrew, J. F. Gent, Y. Kong et al., "Association of sputum microbiota profiles with severity of community-acquired pneumonia in children," *BMC Infectious Diseases*, vol. 16, no. 1, 2016.
- [26] S. M. Teo, D. Mok, K. Pham et al., "The infant nasopharyngeal microbiome impacts severity of lower respiratory infection and risk of asthma development," *Cell Host & Microbe*, vol. 17, no. 5, pp. 704–715, 2015.
- [27] J. J. Kozich, S. L. Westcott, N. T. Baxter, S. K. Highlander, and P. D. Schloss, "Development of a dual-index sequencing strategy and curation pipeline for analyzing amplicon sequence data on the MiSeq Illumina sequencing platform," *Applied and Environmental Microbiology*, vol. 79, no. 17, pp. 5112–5120, 2013.
- [28] J. G. Caporaso, J. Kuczynski, J. Stombaugh et al., "QIIME allows analysis of high-throughput community sequencing data," *Nature Methods*, vol. 7, no. 5, pp. 335–336, 2010.
- [29] H. Wang, W. Dai, C. Qiu et al., "Mycoplasma pneumoniae and Streptococcus pneumoniae caused different microbial structure and correlation network in lung microbiota," *Journal of Thoracic Disease*, vol. 8, no. 6, pp. 1316–1322, 2016.
- [30] I. Letunic and P. Bork, "Interactive tree of life (iTOL) v3: an online tool for the display and annotation of phylogenetic and other trees," *Nucleic Acids Research*, vol. 44, no. 1, pp. W242–W245, 2016.
- [31] S. Subramanian, S. Huq, T. Yatsuneneko et al., "Persistent gut microbiota immaturity in malnourished Bangladeshi children," *Nature*, vol. 510, no. 7505, pp. 417–421, 2014.
- [32] W. A. de Steenhuijsen Piters, E. A. Sanders, and D. Bogaert, "The role of the local microbial ecosystem in respiratory health and disease," *Philosophical Transactions of the Royal Society B: Biological Sciences*, vol. 370, no. 1675, 2015.
- [33] E. S. Gollwitzer and B. J. Marsland, "Impact of Early-Life Exposures on Immune Maturation and Susceptibility to Disease," *Trends in Immunology*, vol. 36, no. 11, pp. 684–696, 2015.
- [34] G. Biesbroek, E. Tsvitvadze, E. A. M. Sanders et al., "Early respiratory microbiota composition determines bacterial succession patterns and respiratory health in children," *American Journal of Respiratory and Critical Care Medicine*, vol. 190, no. 11, pp. 1283–1292, 2014.
- [35] S. J. Siegel, A. M. Roche, and J. N. Weiser, "Influenza promotes pneumococcal growth during coinfection by providing host sialylated substrates as a nutrient source," *Cell Host & Microbe*, vol. 16, no. 1, pp. 55–67, 2014.
- [36] M. Yan, S. J. Pamp, J. Fukuyama et al., "Nasal microenvironments and interspecific interactions influence nasal microbiota complexity and *S. aureus* carriage," *Cell Host & Microbe*, vol. 14, no. 6, pp. 631–640, 2013.
- [37] I. Arnit, M. Garber, N. Chevrier et al., "Unbiased reconstruction of a mammalian transcriptional network mediating pathogen responses," *Science*, vol. 326, no. 5950, pp. 257–263, 2009.
- [38] N. Chevrier, P. Mertins, M. N. Artyomov et al., "Systematic discovery of TLR signaling components delineates viral-sensing circuits," *Cell*, vol. 147, no. 4, pp. 853–867, 2011.
- [39] C. M. Bassis, J. R. Erb-Downward, R. P. Dickson et al., "Analysis of the upper respiratory tract microbiotas as the source of the lung and gastric microbiotas in healthy individuals," *mBio*, vol. 6, no. 2, Article ID e00037-15, 2015.
- [40] E. S. Charlson, K. Bittinger, A. R. Haas et al., "Topographical continuity of bacterial populations in the healthy human respiratory tract," *American Journal of Respiratory and Critical Care Medicine*, vol. 184, no. 8, pp. 957–963, 2011.
- [41] C. Bellinghausen, G. G. U. Rohde, P. H. M. Savelkoul, E. F. M. Wouters, and F. R. M. Stassen, "Viral-bacterial interactions in the respiratory tract," *Journal of General Virology*, vol. 97, no. 12, pp. 3089–3102, 2016.
- [42] M. M. Pettigrew, A. S. Laufer, J. F. Gent, Y. Kong, K. P. Fennie, and J. P. Metlay, "Upper respiratory tract microbial communities, acute otitis media pathogens, and antibiotic use in healthy and sick children," *Applied and Environmental Microbiology*, vol. 78, no. 17, pp. 6262–6270, 2012.
- [43] S. Nakamura, K. M. Davis, and J. N. Weiser, "Synergistic stimulation of type I interferons during influenza virus coinfection promotes Streptococcus pneumoniae colonization in mice," *The Journal of Clinical Investigation*, vol. 121, no. 9, pp. 3657–3665, 2011.
- [44] E. T. Zemanick, B. D. Wagner, C. E. Robertson et al., "Airway microbiota across age and disease spectrum in cystic fibrosis," *European Respiratory Journal*, vol. 50, no. 5, p. 1700832, 2017.
- [45] P. N. Luna, K. Hasegawa, N. J. Ajami et al., "The association between anterior nares and nasopharyngeal microbiota in infants hospitalized for bronchiolitis," *Microbiome*, vol. 6, no. 1, 2018.
- [46] C. J. Heneghan, I. Onakpoya, M. A. Jones et al., "Neuraminidase inhibitors for influenza: A systematic review and meta-analysis of regulatory and mortality data," *Health Technology Assessment*, vol. 20, no. 42, pp. 1–242, 2016.
- [47] M. E. Bonomo and M. W. Deem, "Predicting influenza h3n2 vaccine efficacy from evolution of the dominant epitope," *Clin Infect Dis*, no. vol, 2018.